



Photon-photon correlation of condensed light in a microcavity

Yijun Tang ¹, Himadri S. Dhar ², Rupert F. Oulton,¹ Robert A. Nyman ¹, and Florian Mintert^{1,3}

¹*Physics Department, Blackett Laboratory, Imperial College London, Prince Consort Road, SW7 2AZ, United Kingdom*

²*Department of Physics, Indian Institute of Technology Bombay, Mumbai 400076, India*

³*Helmholtz-Zentrum Dresden-Rossendorf, Bautzner Landstraße 400, 01328 Dresden, Germany*



(Received 25 October 2023; accepted 20 March 2024; published 23 April 2024)

The study of temporal coherence in a Bose-Einstein condensate of photons can be challenging, especially in the presence of correlations between the photonic modes. In this work, we use a microscopic, multimode model of photonic condensation inside a dye-filled microcavity and the quantum regression theorem to derive an analytical expression for the equation of motion of the photon-photon correlation function. This allows us to derive the coherence time of the photonic modes and identify a nonmonotonic dependence of the temporal coherence of the condensed light with the cutoff frequency of the microcavity.

DOI: [10.1103/PhysRevA.109.043713](https://doi.org/10.1103/PhysRevA.109.043713)

I. INTRODUCTION

A defining property of a Bose-Einstein condensate (BEC) is the macroscopic coherence exhibited by the particles in the lowest energy mode—a feature that allows the condensate to behave like a massive quantum wave [1,2]. While features such as thermal equilibrium and large population of the ground state are the telltale signatures of a BEC, onset of quantum coherence can be a defining characteristic of condensates that do not thermalize completely and essentially operate out of equilibrium, such as exciton-polaritons [3,4] and photons [5–8]. As such, theoretical and experimental investigation of coherence in both equilibrium and nonequilibrium condensates plays an important role in characterizing the properties of these macroscopic states. Over the years, coherence of BEC has been observed using interference experiments with ultracold atoms [9,10]. Moreover, coherence in condensates of excitons-polaritons [11] and organic polaritons [12] have also been reported, while spontaneous phase selection [13] and spatiotemporal coherence [14,15] has been observed in photonic condensates.

The photonic Bose-Einstein condensates formed inside a dye-filled microcavity is driven-dissipative in nature, sustained by a detailed balance between the rate at which the dye molecules are incoherently driven and losses of molecular and photonic excitation in the system. The thermalization of the photon gas inside the microcavity is due to the vibrational states of the dye molecule, which allow thermal equilibration of photons via energy-dependent absorption and emission processes. From a physical perspective, one of the central differences between a photonic BEC and a laser is the rate of thermalization it is operating under. While a photonic BEC works in a near-equilibrium regime, close to thermal equilibrium with the dye molecules, a laser operates at a much lower thermalization rate and is firmly in the nonequilibrium

regime. As such, macroscopic occupation of photons occurs in the lowest energy mode in a photon condensate, irrespective of the gain, whereas for a laser the large population typically corresponds to the mode with the highest gain. Between these regimes lie exotic phases of light that exhibit strong multimode properties [16], nonstationary kinetics [17,18], and possible vortex-like features [19].

A key characteristic of Bose-Einstein condensates that operate in the near-equilibrium regime is the spatiotemporal coherence. While condensates of exciton-polaritons exhibit significant interparticle interactions, which lead to phase coherence [20] and superfluid behavior in the system [21], photons in a BEC do not interact strongly with each other [22,23]. Instead, coherence is created from indirect interaction of photons with the dye molecules, mediated via stimulated emissions [24]. This leads to coherence properties such as symmetry-broken phase coherence [13], grand-canonical photon statistics [25], and transition from short-range to long-range spatial order across the condensation threshold [14,15], which has been experimentally observed. While phase coherence is generally well understood in these systems, studies on temporal coherence that are consistent with experimental results have been limited [14,16].

The properties of a photon condensate are well described by a microscopic model [26], derived from the light-matter interaction between a multimode cavity and an ensemble of emitters that represents the electronic and vibrational states of the dye molecules. The model can perfectly capture the thermalization [27] and near-equilibrium properties [28] of the photon gas in the cavity, and also highlight features such as decondensation [29] and noncritical slowing down of dynamics [30]. First-order correlation function and the photon linewidth [27] based on a single-mode model predict a perfect temporal coherence in the condensed mode, consistent with the Schawlow-Townes limit at large photon numbers [31]. While the theoretical results are in agreement with experimental observations in the vicinity of the BEC threshold [14,16], it exhibits significant deviation at higher photon numbers.

In this work, we derive the equation of motion of the photon-photon or the first-order correlation function of the

Published by the American Physical Society under the terms of the Creative Commons Attribution 4.0 International license. Further distribution of this work must maintain attribution to the author(s) and the published article's title, journal citation, and DOI.

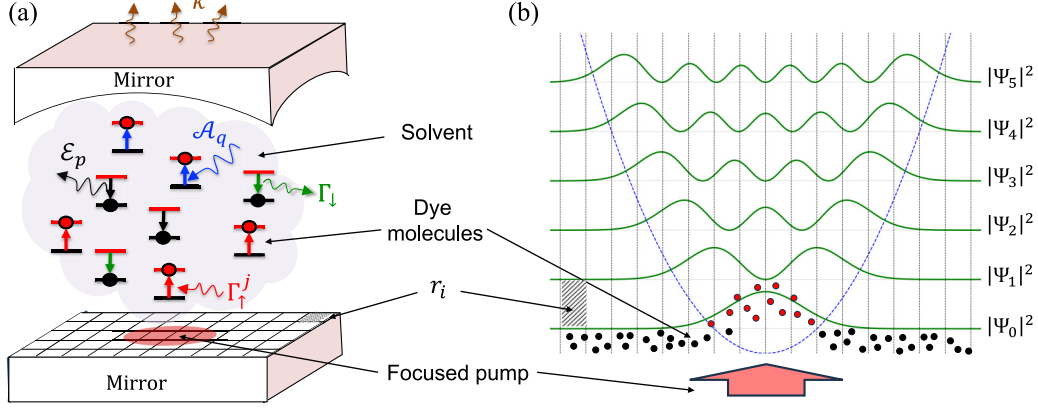


FIG. 1. Illustration of a photon BEC setup. (a) A microcavity, formed using a pair of curved and flat mirrors, filled with dye molecules (two-level systems) in a solvent (gray cloud). The figure illustrates different processes such as emission (\mathcal{E}_p), absorption (\mathcal{A}_q), photon loss (κ), and loss of molecular excitation (Γ_\downarrow). The cavity plane can be divided into a grid, with each box indexed as \mathbf{r}_i (shaded region), and focused pumping (Γ_\uparrow^j) at the center (red region). (b) A one-dimensional portrayal of the BEC setup showing the grids and the probability density $|\Psi_p|^2$ for the first six cavity modes. The unexcited (black) and excited (red) are uniformly distributed in the plane (three per grid). The excited molecules are located closer to the pump spot.

photon gas inside a dye-filled microcavity, especially when interactions between the different cavity modes are explicitly taken into account. Such a model already provides great insight into the role of spatial coherence in the kinetics of the condensed light in the cavity [19,28]. Our focus here is on the temporal coherence of the condensed light, and by using the quantum regression theorem, we derive an analytical expression for the equation of motion of the photon-photon correlation. This allows us to study the temporal coherence or the coherence time of light inside the cavity for different system parameters.

The paper is arranged as follows. After the Introduction in Sec. I, we study the multimode model in Sec. II, and derive the rate equations for the photon correlations and molecular excitations. In Sec. III, we represent the photon-photon correlations in terms of the coefficients of the density matrix of the system. In Sec. IV, the time derivative of these coefficients is obtained to ultimately derive the equation of motion of the photon-photon correlation in Sec. V. In Sec. VI, the time evolution of the correlation is numerically studied and the coherence time of the condensed light for different cutoff frequencies and pumping rate are presented. The results are discussed in Sec. VII.

II. THEORETICAL MODEL

The interaction of photons with the dye molecules inside a microcavity can be studied using a microscopic model [26]. In its most general form, the theoretical model is valid for multiple cavity modes and also takes into account finite inter-mode correlations [28]. The dynamics of the quantum system is governed by the following master equation:

$$\begin{aligned} \frac{d\rho}{dt} = & -i[\hat{H}_0, \hat{\rho}] + \frac{1}{2} \sum_{i,p} (\kappa L[\hat{a}_p] + \Gamma_\uparrow^i L[\hat{\sigma}_i^+] + \Gamma_\downarrow L[\hat{\sigma}_i^-]) \\ & + \frac{1}{2} \sum_{i,p,q} (\Psi_{p,q}^i \{ \mathcal{A}_q [\hat{a}_q \hat{\sigma}_i^+ \rho, \hat{a}_p^\dagger \hat{\sigma}_i^-] + \mathcal{E}_p [\hat{a}_p^\dagger \hat{\sigma}_i^- \rho, \hat{a}_q \hat{\sigma}_i^+] \} \\ & + \text{H.c.}), \end{aligned} \quad (1)$$

where $\hat{H}_0 = \sum_p \delta_p \hat{a}_p^\dagger \hat{a}_p$ is the bare energy of the cavity photons, and $L[\hat{x}] = 2\hat{x}\rho\hat{x}^\dagger - \{\hat{x}^\dagger\hat{x}, \rho\}$, with $\{\cdot\}$ being the anticommutator. Here, \hat{a}_p (\hat{a}_p^\dagger) is the annihilation (creation) operator of photons in the p th cavity mode, and κ is the rate at which it is lost from the cavity. The Pauli operators σ_i^\pm denote the electronic states of the dye molecule at location \mathbf{r}_i in the cavity plane, which is pumped at a rate Γ_\uparrow^i , but decays with a uniform rate Γ_\downarrow to noncavity modes. The pump is focused at the center of the cavity and has a Gaussian profile. An illustration of the setup, highlighting the different processes, is shown in Fig. 1.

The modes of the cavity are determined by the experimental setup. The frequency ω_0 of the lowest cavity mode, referred to as cutoff frequency, is determined by the cavity length; the mode spacing $\Delta\omega$ is given by the curvature of the cavity mirrors [16]. The lowest energy mode ω_0 corresponds to the cutoff frequency of the cavity, which is adjusted by the cavity length, and the mode spacing $\Delta\omega$ is given by the curvature of one of the mirrors [16]. The frequency of cavity mode p is then given by $\omega_p = \omega_0 + p\Delta\omega$. The rate of absorption and emission of photons in the p th mode are given by \mathcal{A}_p and \mathcal{E}_p , respectively, and can either be calculated [27] or estimated from experimental data of the absorption cross section [32]. Moreover, these rates are known to follow the Kennard-Stepanov relation [33–35], $\mathcal{A}_p = \mathcal{E}_p e^{-\beta\delta_p}$, with $\delta_p = \omega_{\text{ZPL}} - \omega_p$, where ω_{ZPL} is the zero-phonon line or the transition frequency between the electronic levels of a dye molecule. The choice of cutoff frequency is important in choosing the appropriate absorption-emission spectrum that allows for near-equilibrium conditions for photons to thermalize and condense [26]. The expression $\Psi_{p,q}^i = \psi_p(\mathbf{r}_i)\psi_q(\mathbf{r}_i)$ gives the overlap of the spatial profile of modes p and q at position \mathbf{r}_i , where ψ_k is the mode function of the k th mode given by the Hermite-Gauss functions. The number of molecules and modes are denoted by N and M , respectively, and the molecules are assumed to be uniformly distributed inside the cavity.

The dynamics as well as the steady behavior of the cavity modes and the molecular excitation can be studied in terms of

the equations of motion of the relevant observables, such as the mode population or photon correlation, obtained from the above master equation. In most cases, it is easier to work with rate equations compared to directly solving the density matrix, especially when the system contains a large number of modes and an inhomogeneous distribution of molecular excitations.

On the other hand, equations of motion for observables such as the mode population $\langle \hat{a}_p^\dagger \hat{a}_p \rangle$ and the molecular excitation $\langle \sigma_i^+ \sigma_i^- \rangle$ or two-mode correlation function $\langle \hat{a}_p^\dagger \hat{a}_q \rangle$ can be computed with relatively little computational resources when certain approximations are taken into consideration. First, it is helpful to use the fact that coupling between different dye molecules has been neglected on account of the incessant collision between the molecules of the dye and the solvent, which quickly decoheres any intermolecular coherence. Secondly, one can invoke the semiclassical approximation such that correlations between molecules and photons can be factorized, i.e., $\langle \sigma_i^+(t) \hat{a}_q(t) \rangle \approx \langle \sigma_i^+(t) \rangle \langle \hat{a}_q(t) \rangle$. This is typically a good approximation when the number of emitters in a cavity is large, which is true in the case of a dye-filled microcavity, where the number of dye molecules inside the microcavity is very large.

The photon population and correlations can be written as a matrix \mathbf{n} , with elements $n_{pq}(t) = \langle \hat{a}_p^\dagger(t) \hat{a}_q(t) \rangle$, and the molecular excitation fraction as a vector \mathbf{f} with elements $f_i = \sum_j \langle \sigma_j^+ \sigma_j^- \rangle \delta(\mathbf{r}_i - \mathbf{r}_j)$. The semiclassical equations of motion for \mathbf{n} and \mathbf{f} are then given by

$$\dot{\mathbf{n}} = \left(i\boldsymbol{\Omega} - \frac{\kappa}{2} \right) \mathbf{n} + \{\mathbf{f}^+ \mathbf{E}(\mathbf{n} + \mathbb{1}) - \mathbf{f}^- \mathbf{A}\mathbf{n}\} + \text{H.c.}, \quad (2)$$

$$\dot{\mathbf{f}} = -\{\Gamma_\downarrow + 2\tilde{\mathbf{E}}\}\mathbf{f} + \{\Gamma_\uparrow + 2\tilde{\mathbf{A}}\}(\mathbf{1} - \mathbf{f}), \quad (3)$$

where \mathbf{f}^+ and \mathbf{f}^- have elements $f_{pq}^+ = \sum_i f_i \Psi_{pq}^i$ and $f_{pq}^- = \sum_i (1 - f_i) \Psi_{pq}^i$, respectively. \mathbf{A} , \mathbf{E} , and $\boldsymbol{\Omega}$ are diagonal matrices with elements \mathcal{A}_p , \mathcal{E}_p , and ω_p , respectively. Γ_\uparrow is a diagonal matrix with entries Γ_\uparrow^i and $\mathbf{1}$ is a vector with all elements equal to unity. The matrices $\tilde{\mathbf{E}}$ and $\tilde{\mathbf{A}}$ are diagonal with elements $\text{Tr}[\Phi_i \mathbf{E}(\mathbf{n} + \mathbb{1})]$ and $\text{Tr}[\Phi_i \mathbf{n} \mathbf{A}]$, respectively, where Φ_i has the same dimension as \mathbf{n} and has elements Ψ_{pq}^i . Importantly, Eqs. (2) and (3) allow for the computation of the photon correlation function $\langle \hat{a}_p^\dagger(t) \hat{a}_q(t) \rangle$ at time t , as well as at the steady state of the system, for a given set of system parameters.

III. PHOTON-PHOTON CORRELATION FUNCTION

The primary focus of the work is to calculate the first-order correlation function, which would allow for the estimation of the spectral linewidth, as well as the temporal coherence of the multimode photon gas inside the dye-filled microcavity. The key quantity of interest is the photon-photon correlation,

$$c_{pq}(t_2 - t_1) = \langle \hat{a}_p^\dagger(t_2) \hat{a}_q(t_1) \rangle, \quad (4)$$

where p and q denote the cavity modes. For most experiments involving the investigation of spatiotemporal coherence, the initial state of the system at t_1 is the steady state ρ_{ss} . As such, only the time difference, $t = t_2 - t_1$, is relevant, and the two-time correlation reduces to $c_{pq}(t) = \langle \hat{a}_p^\dagger(t) \hat{a}_q(0) \rangle$, where one can set the initial time $t_1 = 0$, and $t_2 = t$. Therefore, the

two-time correlation can now be calculated using the term $\text{Tr}[\hat{a}_p^\dagger(t) \hat{a}_q(0) \rho_{ss}]$.

The correlation function can be calculated using the quantum regression theorem [36,37], which allows for setting up an equation of motion for the two-time correlation. The function $\langle \hat{a}_p^\dagger(t) \hat{a}_q(0) \rangle$ can be considered as the time evolution of the term $\langle \hat{a}_p^\dagger \rangle$, governed by the master equation given in Eq. (1), however, with the initial state given by $\rho'(0) = \hat{a}_q \rho_{ss}$. In other words, using the regression theorem, we have the relation

$$c_{pq}(t) = \langle \hat{a}_p^\dagger \rangle = \text{Tr}[\hat{a}_p^\dagger \rho'] = \text{Tr}[\hat{a}_p^\dagger(t) \hat{a}_q(0) \rho_{ss}]. \quad (5)$$

Similar approaches have been used to derive the first-order [27] and second-order correlation function [18]. But, these are mostly restricted to just single-mode systems, where there are no interactions arising from intermode correlations and the overall dynamics is fairly simple.

To apply the regression theorem, it is helpful to work with the density matrix formalism, which can be written in an expanded form using an appropriate orthonormal basis. For M photon modes and N molecules inside the cavity, one such basis is $\{|\underline{n}, \underline{s}\rangle\}$, where $|\underline{n}\rangle = |n_0 n_1 \dots n_p \dots n_M\rangle$ with n_p being the population of the p th mode. Similarly, $|\underline{s}\rangle = |s_1 s_2 \dots s_j \dots s_N\rangle$ is the molecular excitation state, where s_i can take values 0 or 1, depending on whether the i th molecule is excited or not. Thus, the density matrix ρ can then be expressed in this basis as

$$\rho = \sum_{\underline{n}, \underline{n}', \underline{s}} C_{\underline{n}, \underline{n}', \underline{s}} |\underline{n}\rangle \langle \underline{n}'| \otimes |\underline{s}\rangle \langle \underline{s}|, \quad (6)$$

where $|\underline{n}, \underline{s}\rangle \langle \underline{n}', \underline{s}'| = |\underline{n}\rangle \langle \underline{n}'| \otimes |\underline{s}\rangle \langle \underline{s}'|$, based on the fact that there is no coherence between the molecules and the semiclassical approximation is valid. Now, the diagonal elements of ρ are those that satisfy $\underline{n} = \underline{n}'$ and the off-diagonal terms are for $\underline{n} \neq \underline{n}'$. In general, $\underline{n}, \underline{n}' \geq 0$, which means $n_p \geq 0 \forall p$ and implies that mode population is nonnegative. As such, the following rearrangement of terms can be made:

$$\begin{aligned} \sum_{\underline{n}' \geq 0} \sum_{\underline{n} \geq 0} |\underline{n}\rangle \langle \underline{n}'| &= \sum_{\underline{n}' \geq 0} \sum_{\underline{n}' - \underline{k} \geq 0} |\underline{n}' - \underline{k}\rangle \langle \underline{n}'| \\ &\equiv \sum_{\underline{k} \leq \underline{n}} \sum_{\underline{n} \geq 0} |\underline{n} - \underline{k}\rangle \langle \underline{n}|. \end{aligned} \quad (7)$$

So, ρ can now be rearranged in terms of $|\underline{n} - \underline{k}\rangle \langle \underline{n}|$, where $\underline{n}' - \underline{n} = \underline{k}$,

$$\rho = \sum_{\underline{k}} \left(\sum_{\underline{n}, \underline{s}} R_{\underline{n}, \underline{s}}^{\underline{k}} |\underline{n} - \underline{k}\rangle \langle \underline{n}| \otimes |\underline{s}\rangle \langle \underline{s}| \right), \quad (8)$$

and $R_{\underline{n}, \underline{s}}^{\underline{k}} = \langle \underline{n} - \underline{k}, \underline{s} | \rho | \underline{n}, \underline{s} \rangle$. Note that \underline{k} can be nonpositive and the above expression can be thought of as representing the density matrix by summing the k th diagonal terms.

The two-time correlation can now be computed by taking the trace $\text{Tr}[\hat{a}_p^\dagger \rho']$, where

$$\rho' = \hat{a}_q \rho = \sum_{\underline{k}, \underline{n}, \underline{s}} P_{\underline{n}, \underline{s}}^{\underline{k}} |\underline{n} - \underline{k}\rangle \langle \underline{n}| \otimes |\underline{s}\rangle \langle \underline{s}|, \quad (9)$$

where we expand ρ' similarly as in Eq. (8) with a new set of coefficients $\{P_{\underline{n}, \underline{s}}^{\underline{k}}\}$ which are related to the steady-state coef-

ficients by $P_{\underline{n},\underline{s}}^{k_p}(0) = \sqrt{n_q - k_q + 1} R_{\underline{n},\underline{s}}^{k-k_q}$, where k_q is defined as a vector with the q th term as unity and zero elsewhere. As such, we obtain the following expression:

$$\begin{aligned} c_{pq}(t) &= \text{Tr}[\hat{a}_p^\dagger \rho'] = \text{Tr} \left[\hat{a}_p^\dagger \sum_{\underline{k}, \underline{n}, \underline{s}} P_{\underline{n},\underline{s}}^k |\underline{n} - \underline{k}\rangle \langle \underline{n}| \otimes |\underline{s}\rangle \langle \underline{s}| \right] \\ &= \sum_{\underline{n}, \underline{s}} \left(\sum_{\underline{k}, \underline{n}'} \sqrt{n_p - k_p + 1} P_{\underline{n},\underline{s}}^k \langle \underline{n}' | \underline{n} - \underline{k} + \underline{k}_p \rangle \right. \\ &\quad \left. \times \langle \underline{n} | \underline{n}' \rangle \right) \otimes \sum_{\underline{s}'} \langle \underline{s}' | \underline{s} \rangle \langle \underline{s} | \underline{s}' \rangle \\ &= \sum_{\underline{n}, \underline{s}} \sqrt{n_p} P_{\underline{n},\underline{s}}^{k_p}. \end{aligned} \quad (10)$$

This gives us a time evolution of the photon-photon correlation in terms of the coefficients

$$\dot{c}_{pq}(t) = \frac{d}{dt} \langle \hat{a}_p^\dagger(t) \hat{a}_q(0) \rangle = \sum_{\underline{n}, \underline{s}} \sqrt{n_p} \dot{P}_{\underline{n},\underline{s}}^{k_p}. \quad (11)$$

IV. CALCULATION OF COEFFICIENTS

The estimation of the photon-photon correlation now depends on finding the solution to Eq. (11), which is obtained by finding the terms $\dot{P}_{\underline{n},\underline{s}}^{k_p}$. In particular, the above time derivative needs to be expressed as a function of the coefficients defined in Eqs. (8) and (9), which gives the expression for the operator ρ' in terms of $\{P_{\underline{n},\underline{s}}^{k_p}\}$. Hence, to obtain the time derivative of the two-time correlation, the natural step is to calculate the derivative of the operator ρ' using the master equation in Eq. (1). In particular, the different terms in the master equation need to be investigated for their contribution to the time derivative, starting from the Hamiltonian \hat{H}_0 to the Lindblad terms $L[\hat{\sigma}_i^\pm]$ and $L[\hat{a}_p]$. For example, contribution from \hat{H}_0 in finding the relevant terms in $\dot{\rho}$ will simply come from

$$\dot{\rho} \stackrel{\hat{H}_0}{=} -i[\hat{H}_0, \rho] = -i(\hat{H}_0 \rho - \rho \hat{H}_0), \quad (12)$$

where $\hat{H}_0 = \sum_m \hat{a}_m^\dagger \hat{a}_m$. Here are the contributions from the different terms in the master equation:

(i) \hat{H}_0 contribution

$$\dot{P}_{\underline{n},\underline{s}}^{k_p} \stackrel{\hat{H}_0}{\longrightarrow} i\delta_p P_{\underline{n},\underline{s}}^{k_p}. \quad (13)$$

(ii) $L[\hat{a}_p]$ contribution

$$\dot{P}_{\underline{n},\underline{s}}^{k_p} \stackrel{L[\hat{a}_p]}{\longrightarrow} \sum_m \kappa \left[C_0(m) P_{\underline{n}+\underline{k}_m, \underline{s}}^{k_p} - \left(n_m - \frac{\delta_{p,m}}{2} \right) P_{\underline{n},\underline{s}}^{k_p} \right], \quad (14)$$

where $C_0(m) = \sqrt{(n_m + 1)(n_m + 1 - \delta_{p,m})}$. Note that κ describes the loss rate for all cavity modes, and a state \underline{n} can lose a photon in mode m and thus change into $\underline{n} - \underline{k}_m$, where \underline{k}_m (as defined earlier) is a vector with the m th element as 1 and 0 everywhere else. Conversely, a photon population \underline{n} can come from state $\underline{n} + \underline{k}_m$ by losing a photon in mode m . As such, these states have probability $P_{\underline{n}+\underline{k}_m, \underline{s}}^{k_p}$.

(iii) $L[\hat{\sigma}_i^\pm]$ contribution

$$\dot{P}_{\underline{n},\underline{s}}^{k_p} \stackrel{L[\hat{\sigma}_i^\pm]}{\longrightarrow} \sum_{i, \forall s_i=1} \Gamma_\uparrow^i P_{\underline{n},\underline{s}-\underline{s}_i}^{k_p} - \tilde{\Gamma}_\uparrow P_{\underline{n},\underline{s}}^{k_p}, \quad (15)$$

where $\tilde{\Gamma}_\uparrow = \sum_{i, \forall s_i=0} \Gamma_\uparrow^i$ and \underline{s}_i is a vector with the i th element as 1 and 0 everywhere else. As Γ_\uparrow^i is the pumping rate, it excites the state \underline{s} to $\underline{s} + \underline{s}_i$ by exciting the i th molecule. Similarly, a state \underline{s} may be pumped from a state $\underline{s} - \underline{s}_i$ with probability $P_{\underline{n},\underline{s}-\underline{s}_i}^{k_p}$. The term $L[\hat{\sigma}_i^-]$, being the decay of a molecule with rate Γ_\uparrow , simply produces a reverse-state transformation. A more detailed description of the above transformations is shown in Appendix A.

(iv) \mathcal{A}_m and $\mathcal{E}_{m'}$ contribution

$$\begin{aligned} \dot{P}_{\underline{n},\underline{s}}^{k_p} &\stackrel{\mathcal{A}_m}{\longrightarrow} \sum_{m, m'} \frac{\mathcal{A}_{m'}}{2} \left[C_1 \left(\sum_{i, \forall s_i=1} \Psi_{m, m'}^i P_{\underline{n}+\underline{k}_m, \underline{s}-\underline{s}_i}^{k_p - \underline{k}_{m'} + \underline{k}_m} \right) \right. \\ &\quad \left. - C_2 \left(\sum_{i, \forall s_i=0} \Psi_{m, m'}^i \right) P_{\underline{n}, \underline{s}}^{k_p - \underline{k}_{m'} + \underline{k}_m} \right], \end{aligned} \quad (16)$$

where $C_1 = \sqrt{(n_{m'} - \delta_{p, m'} + 1)(n_m + 1)}$ and $C_2 = \sqrt{(n_m - \delta_{m, p} + 1 - \delta_{m, m'})(n_{m'} - \delta_{p, m'})}$.

Note that the process of absorption and emission, as governed by \mathcal{A}_m and $\mathcal{E}_{m'}$ in Eq. (1), gives rise to intermode correlations. In the case of $m = m'$ the mode is coupled to itself. Mathematically, this is a state with probability $P_{\underline{n}, \underline{s}}^{k_p}$, which upon absorption of a photon in mode m by the i th molecule at location \mathbf{r}_i will transform to a state with probability $P_{\underline{n}+\underline{k}_m, \underline{s}-\underline{s}_i}^{k_p}$. Now, including $m \neq m'$ introduces intermode correlations, which reveals itself in the coupling of different \underline{k}_i terms. For instance, \underline{k}_p in the derivative on the left-hand side is connected to the $\underline{k}_p - \underline{k}_{m'} + \underline{k}_m$ on the right for all m and m' . Similar calculations can also be done for transformations arising from the emission term $\mathcal{E}_{m'}$. The contribution from the Hermitian conjugates in Eq. (1) are calculated in a similar manner.

Now, the full expression of $\dot{P}_{\underline{n},\underline{s}}^{k_p}$ is simply the sum of the different contributions, which gives us a general relation of the time derivative to the set $\{P_{\underline{n},\underline{s}}^{k_p}\}$.

V. EQUATION OF MOTION

In Eq. (11), we represent the time derivative of the two-time correlation function $\dot{c}_{pq}(t) = \frac{d}{dt} \langle \hat{a}_p^\dagger(t) \hat{a}_q(0) \rangle$ in terms of the rate of change of the probabilities $\dot{P}_{\underline{n},\underline{s}}^{k_p}$. Moreover, in Eqs. (13)–(16), we derived the time derivatives in terms of the probabilities $\{P_{\underline{n},\underline{s}}^{k_p}\}$. As such, the equation of motion of the two-time correlation function $\langle \hat{a}_p^\dagger(t) \hat{a}_q(0) \rangle$ can now be derived independently of these probabilities, which in practical conditions can be very difficult to estimate.

From Sec. IV, the contributions from the \hat{H}_0 and $L[\hat{a}_p]$ terms in the master equation lead to

$$\frac{d}{dt} \langle \hat{a}_p^\dagger(t) \hat{a}_q(0) \rangle = (i\delta_p - \kappa/2) \langle \hat{a}_p^\dagger(t) \hat{a}_q(0) \rangle, \quad (17)$$

and therefore introduce an oscillatory and a decay term in the equation of motion. The terms related to pumping and

decay of molecules in the system, given by $L[\sigma_i^\pm]$, do not contribute to the photon correlation. However, the absorption and emission terms, given by \mathcal{A}_m and $\mathcal{E}_{m'}$, make a significant contribution to the equation of motion. For \mathcal{A}_m this is given by

$$\frac{d}{dt} \langle \hat{a}_p^\dagger(t) \hat{a}_q(0) \rangle = - \sum_{\underline{n}, \underline{s}, m} \frac{\mathcal{A}_m \sqrt{n_m}}{2} \left(\sum_{i, \forall s_i=0} \Psi_{p,m}^i \right) P_{\underline{n}, \underline{s}}^{k_m}. \quad (18)$$

The contribution from $\mathcal{E}_{m'}$ is given simply by replacing the absorption term with emission, the index m by m' , and the summation over all $s_i = 1$. An extended derivation of Eq. (18) is shown in Appendix B.

Importantly, the contributions from \mathcal{A}_m and $\mathcal{E}_{m'}$ still contain coefficients $P_{\underline{n}, \underline{s}}^{k_m}$. A useful condition to use at this point is the semiclassical approximation discussed in Sec. II, which factorizes the correlation between photons and molecules. This leads to $P_{\underline{n}, \underline{s}}^{k_p} \approx P_{\underline{n}}^{k_p} P_{\underline{s}}$, where one can interpret $P_{\underline{s}}$ to be probability for molecules to have an excitation profile described by \underline{s} . As such, Eq. (10) can be written as

$$\begin{aligned} c_{pq}(t) &= \langle \hat{a}_p^\dagger(t) \hat{a}_q(0) \rangle = \sum_{\underline{n}, \underline{s}} \sqrt{n_p} P_{\underline{n}, \underline{s}}^{k_p} \\ &= \sum_{\underline{n}} \sqrt{n_p} P_{\underline{n}}^{k_p} \sum_{\underline{s}} P_{\underline{s}} = \sum_{\underline{n}} \sqrt{n_p} P_{\underline{n}}^{k_p}, \end{aligned} \quad (19)$$

where the sum over probabilities of all possible molecular excitation profiles is unity, i.e., $\sum_{\underline{s}} P_{\underline{s}} = 1$. Now, to simplify the expression in Eq. (18), we use the semiclassical approximation in Eq. (19), such that

$$\begin{aligned} \dot{c}_{pq}(t) &\approx - \sum_{\underline{n}, m} \frac{\mathcal{A}_m \sqrt{n_m}}{2} P_{\underline{n}}^{k_m} \sum_{\underline{s}} \left(P_{\underline{s}} \sum_{i, \forall s_i=0} \Psi_{p,m}^i \right), \\ &= - \sum_m \frac{\mathcal{A}_m}{2} c_{mq}(t) \sum_{\underline{s}} \left(P_{\underline{s}} \sum_{i, \forall s_i=0} \Psi_{p,m}^i \right). \end{aligned} \quad (20)$$

The coefficient $\sum_{\underline{s}} (P_{\underline{s}} \sum_{i, \forall s_i=0} \Psi_{p,m}^i)$ here is not straightforward. It is a sum of the mode function $\Psi_{p,m}^i$ at locations \mathbf{r}_i , where the molecule is not excited as described by the vector $[\underline{s}]$. The above expression can be rewritten as shown in Appendix C, as $\sum_i \Psi_{p,m}^i (1 - f_i)$, where f_i is the probability of finding an excited molecule at location \mathbf{r}_i or equivalently, the excitation fraction. A similar expression can also be obtained from the emission $\mathcal{E}_{m'}$ term.

Therefore, bringing all the terms together, the full equation of motion for the photon-photon correlation is given by

$$\begin{aligned} \frac{d}{dt} \langle \hat{a}_p^\dagger(t) \hat{a}_q(0) \rangle &= (i\delta_p - \kappa/2) \langle \hat{a}_p^\dagger(t) \hat{a}_q(0) \rangle \\ &+ \sum_m \left(\frac{\mathcal{E}_m}{2} f_{mp}^+ - \frac{\mathcal{A}_m}{2} f_{mp}^- \right) \langle \hat{a}_m^\dagger(t) \hat{a}_q(0) \rangle, \end{aligned} \quad (21)$$

where $f_{mp}^+ = \sum_i f_i \Psi_{m,p}^i$ and $f_{mp}^- = \sum_i (1 - f_i) \Psi_{m,p}^i$.

The photon-photon correlation or the first-order correlation function allows for the estimation of the emission spectrum of the cavity and the temporal coherence of the different modes. The time evolution of the correlation function $c_{pq}(t) =$

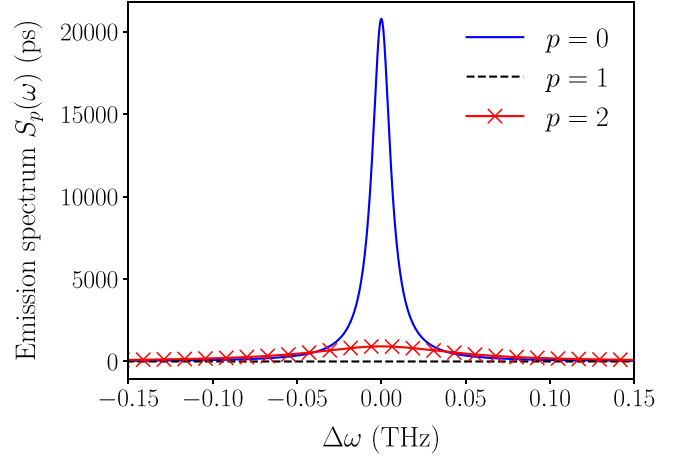


FIG. 2. The emission spectrum of the first few photonic modes. The figure shows the spectral function $S_p(\omega)$, normalized with the initial steady-state population $\langle \hat{a}_p^\dagger(t) \hat{a}_p(t) \rangle$ at $t = 0$, for the ground state $p = 0$ (solid blue line), the first excited $p = 1$ (dashed black line), and the second excited $p = 2$ (red crossed line) modes. The pump is focused at the center, with a width equal to thrice the oscillator length l_0 . The cavity cutoff frequency $\omega_0 \approx 520$ THz, with spacing between two adjacent cavity modes, $\Delta\omega = 1.7$ THz. The rate of loss of cavity photons is equal to $\kappa \approx 0.2$ THz and the absorption (\mathcal{A}_m) and emission (\mathcal{E}_m) rates are calculated from experimental data [32]. The loss of excitations outside the cavity modes is $\Gamma_\downarrow \approx 3 \times 10^{-5}$ THz and pumping rate $\Gamma_\uparrow = 0.2 \times \Gamma_\downarrow$.

$\langle \hat{a}_p^\dagger(t) \hat{a}_q(0) \rangle$ is governed by the equation of motion in Eq. (21), which can be numerically solved for a particular set of system parameters. The initial state of the system, at time $t = 0$, is the steady-state correlation given by $\langle \hat{a}_p^\dagger(0) \hat{a}_q(0) \rangle = \langle \hat{a}_p^\dagger \hat{a}_q \rangle_{ss}$, which is obtained by finding the steady-state solutions of Eqs. (2) and (3) discussed in Sec. II.

VI. TEMPORAL COHERENCE

The temporal coherence of the different photonic modes can be studied from the spectral function of the emitted light from the cavity [38], given by the relation

$$S_p(\omega) = \text{Re} \left[\int_{-\infty}^{\infty} \langle \hat{a}_p^\dagger(t) \hat{a}_p(0) \rangle e^{i\omega t} dt \right], \quad (22)$$

which can be estimated by numerically solving for $\langle \hat{a}_p^\dagger(t) \hat{a}_p(0) \rangle$ using Eq. (21). Figure 2 shows the emission spectrum of the condensed ground state mode $p = 0$, in comparison with the first and second excited modes, $p = 1$ and $p = 2$, respectively. The plots show that the ground state has a much narrower linewidth compared to the higher modes, which implies high temporal coherence in the condensed ground state mode. A notable point is the spectrum of the excited modes. The first excited mode has lower emission than the second excited mode, which implies that the second mode is more populated. This is due to the choice of a Gaussian pump spot focused at the center of the cavity, which tends to excite the even modes, with mode functions that peak at the center. Moreover, the even modes also couple more strongly to the ground state [39].

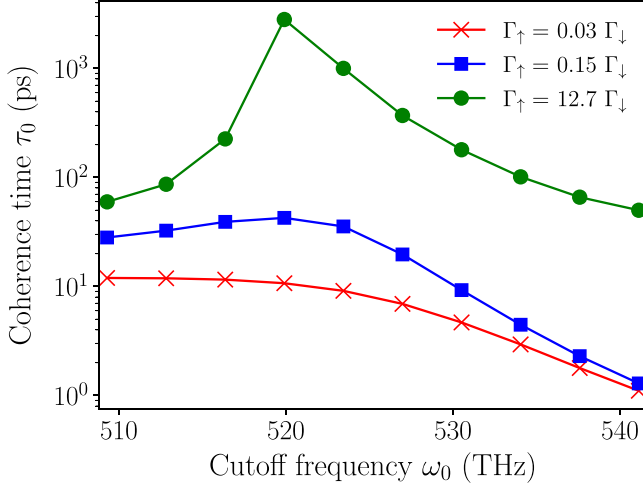


FIG. 3. Variation of temporal coherence with cavity cutoff frequency. The plots show the coherence time of the lowest energy or ground state mode for different cutoff frequencies of the cavity, and for three different pumping rates Γ_\uparrow , in units of Γ_\downarrow . All other system parameters are the same as in Fig. 2.

Importantly, from the close to Lorentzian lineshape in Fig. 2, it can be inferred that the decrease of the correlation function is exponential. Thus, the coherence time τ_p for cavity mode p can be defined as the decay constant of the photon-photon correlation

$$\langle \hat{a}_p^\dagger(t) \hat{a}_p(0) \rangle = c_p(t) = c_p(0) \exp[-t/\tau_p]. \quad (23)$$

Figure 3 shows the variation of the coherence time τ_0 of the lowest energy state with the cutoff frequency ω_0 of the cavity. The cutoff frequency of the cavity is a critical system parameter that not only defines the energy of the lowest cavity mode, but also photon-energy-dependent rates of absorption (\mathcal{A}_p) and emission (\mathcal{E}_p) of photons by the dye molecules inside the cavity. The figure shows that the coherence time is dependent on the cavity cutoff frequency, but does not vary monotonically with change in the cutoff frequency. This is either due to the nonmonotonic variation of thermalization inside the cavity across the chosen range of cutoff frequencies or strong mode competition for molecular excitations. The figure also shows how the coherence time of the ground state depends on the pump power, which controls the total number of photons in the cavity and therefore drives the photon condensation transition.

VII. CONCLUSION

In this work, we derive an equation of motion for the first-order correlation function or the photon-photon correlation for the photon gas inside a dye-filled microcavity. The nonequilibrium model takes into account a multimode photonic cavity, where finite intermode coherences are not completely ignored, which makes the calculations significantly more complex but allows us to compute photon-photon correlations between different modes. Importantly, these relations allow the theoretical and computational investigation of temporal coherence of photon condensates that are consistent with actual experimental findings for a far wider set of parameters [39].

The work opens the door to study more complex behavior of photon correlations and temporal coherence, especially in regimes where strong mode competition for excitation exists. A particular phenomenon of interest is to study how temporal coherence behaves in the regime of multimode condensate, where molecular excitations are clamped by a condensing mode and different modes compete to unclamp the excitation, leading to the phenomenon of decondensation [29]. Moreover, other directions include a more comprehensive study of spatiotemporal correlations in photon condensation under the influence of a nonstationary pump, where phenomena such as vortex-like structure formation [19] and partially coherent light can be engineered.

ACKNOWLEDGMENTS

The authors acknowledge financial support from the European Commission via the PhoQuS project (H2020-FETFLAG-2018-03), Project No. 820392, and the EPSRC (UK) through Grant No. EP/S000755/1. H.S.D. acknowledges financial support from SERB-DST, India, via a Core Research Grant No. CRG/2021/008918 and the Industrial Research & Consultancy Centre, IIT Bombay via grant RD/0521-IRCCSH0-001, No. 2021289.

APPENDIX A: DETAILED CALCULATION OF COEFFICIENTS

The derivation of the coefficients in Sec. IV, which arise due to the different terms in the master equation given by Eq. (1), can be investigated more carefully. The first nontrivial term is $L[\sigma_i^\pm]$, which represents the dynamics due to pumping and decay of molecules as governed by the rates Γ_\uparrow^i and Γ_\downarrow , respectively. These are given by

$$\begin{aligned} & \sum_{\underline{n}, \underline{s}} \hat{P}_{\underline{n}, \underline{s}}^{k_p} |\underline{n} - \underline{k}_p\rangle \langle \underline{n}| \otimes |\underline{s}\rangle \langle \underline{s}| \\ & \xrightarrow{L[\sigma_i^\pm]} -\frac{1}{2} \sum_{i, \underline{n}, \underline{s}} \Gamma_\uparrow^i L[\hat{\sigma}_i^\pm] \hat{P}_{\underline{n}, \underline{s}}^{k_p} |\underline{n} - \underline{k}_p\rangle \langle \underline{n}| \otimes |\underline{s}\rangle \langle \underline{s}|, \\ & = - \sum_{\underline{n}, \underline{s}} \hat{P}_{\underline{n}, \underline{s}}^{k_p} |\underline{n} - \underline{k}_p\rangle \langle \underline{n}| \\ & \quad \otimes \sum_{i, \forall s_i=0} \Gamma_\uparrow^i (|\underline{s}\rangle \langle \underline{s}| - |\underline{s} + \underline{s}_i\rangle \langle \underline{s} + \underline{s}_i|). \end{aligned} \quad (A1)$$

The first term on the right-hand side of Eq. (A1) contains the contribution from the $\{\sigma_i^- \sigma_i^+, \rho\}$ term of the operator $L[\sigma_i^\pm]$ which acts on $|\underline{s}\rangle \langle \underline{s}|$, if and only if $s_i = 0$, i.e., $\sigma_i^- \sigma_i^+ |\underline{s}\rangle \langle \underline{s}| = |\underline{s}\rangle \langle \underline{s}| \sigma_i^- \sigma_i^+ = \delta_{s_i,0} |\underline{s}\rangle \langle \underline{s}|$. Comparing the basis states $|\underline{n} - \underline{k}_p\rangle \langle \underline{n}|$ and $|\underline{s}\rangle \langle \underline{s}|$ on both sides, the coefficient from the first term is $-\hat{P}_{\underline{n}, \underline{s}}^{k_p} \hat{\Gamma}_\uparrow$, where the term $\hat{\Gamma}_\uparrow = \sum_{i, \forall s_i=0} \Gamma_\uparrow^i$, which is the total pump rate at all unexcited sites in the state $|\underline{s}\rangle$.

The second term on the right-hand side arises due to the contribution from the $\sigma_i^+ \rho \sigma_i^-$ term of $L[\sigma_i^\pm]$. Note that this term increases the excitation at locations where the molecules are unexcited or $\sigma_i^+ |\underline{s}\rangle \langle \underline{s}| \sigma_i^- = \delta_{s_i,0} |\underline{s} + \underline{s}_i\rangle \langle \underline{s} + \underline{s}_i|$. This is illustrated in Fig. 4. As such, we obtain the term $\sum_{i, \forall s_i=0} \Gamma_\uparrow^i |\underline{s} + \underline{s}_i\rangle \langle \underline{s} + \underline{s}_i|$, which for any fixed \underline{s} is a summation over all states with one more excitation than \underline{s} . Taking all

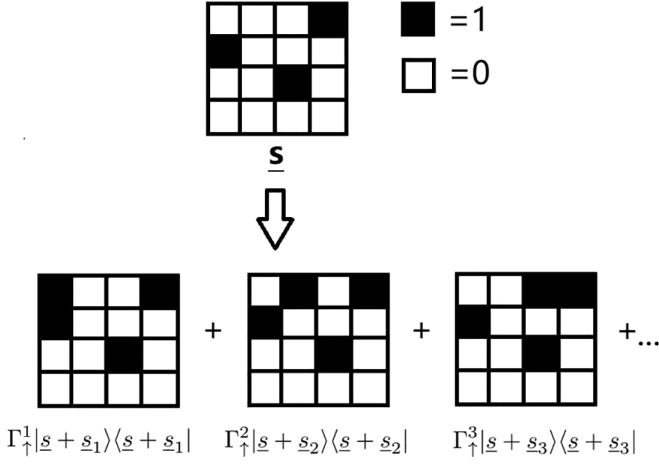


FIG. 4. Visualization of the term $\sum_{i, \forall s_i=0} \Gamma_{\uparrow}^i$ as a square, where each block \mathbf{r}_i denotes a position, and black (white) implying the molecule at the position is excited (nonexcited). For a specific \underline{s} there are associated squares with one more excitation, give by a term Γ_{\uparrow}^j which creates excitation at a new position \mathbf{r}_j , with new basis $|\underline{s} + \underline{s}_j\rangle \langle \underline{s} + \underline{s}_j|$.

\underline{s} into account and noting that there will be no $|\underline{s}\rangle \langle \underline{s}|$, where $s_i = 0 \forall i$, the total contribution of the second term may be rewritten by a simple change of indices,

$$\begin{aligned} & \sum_{\underline{n}, \underline{s}} P_{\underline{n}, \underline{s}}^{k_p} |\underline{n} - \underline{k}_p\rangle \langle \underline{n}| \otimes \sum_{i, \forall s_i=0} \Gamma_{\uparrow}^i |\underline{s} + \underline{s}_i\rangle \langle \underline{s} + \underline{s}_i| \\ & \rightarrow \sum_{\underline{n}, \underline{s}'} P_{\underline{n}, \underline{s}'}^{k_p} |\underline{n} - \underline{k}_p\rangle \langle \underline{n}| \otimes \sum_{i, \forall s'_i=1} \Gamma_{\uparrow}^i |\underline{s}'\rangle \langle \underline{s}'|. \quad (\text{A2}) \end{aligned}$$

The change of indices above is better illustrated in Fig. 5. Now by comparing terms on the left- and right-hand side with

$$\begin{aligned} & \frac{1}{2} \sum_{m, m', i} \Psi_{m, m', i}^i \mathcal{A}_{m'} \hat{a}_m \hat{\sigma}_i^+ \rho \hat{a}_m^\dagger \hat{\sigma}_i^- \\ & = \frac{1}{2} \sum_{m, m', i} \left(\sum_{\underline{n}, \underline{s}} \Psi_{m, m', i}^i \mathcal{A}_{m'} P_{\underline{n}, \underline{s}}^{k_p} \sqrt{(n_{m'} - \delta_{p, m'}) n_m} |\underline{n} - \underline{k}_p - \underline{k}_{m'}\rangle \langle \underline{n} - \underline{k}_m| \otimes \delta_{s_i, 0} |\underline{s} + \underline{s}_i\rangle \langle \underline{s} + \underline{s}_i| \right) \\ & = \frac{1}{2} \sum_{m, m', \underline{n}, \underline{s}} \left[\mathcal{A}_{m'} \sqrt{(n_{m'} - \delta_{p, m'}) n_m} |\underline{n} - \underline{k}_p - \underline{k}_{m'}\rangle \langle \underline{n} - \underline{k}_m| \otimes \sum_{i, \forall s_i=1} \Psi_{m, m', i}^i P_{\underline{n}, \underline{s} - \underline{s}_i}^{k_p} |\underline{s}\rangle \langle \underline{s}| \right] \\ & = \frac{1}{2} \sum_{m, m', \underline{n}', \underline{s}} \left[\mathcal{A}_{m'} \sqrt{(n_{m'}' - \delta_{p, m'} + \delta_{m, m'}) (n_m' + 1)} |\underline{n}' - \underline{k}_p - \underline{k}_{m'} + \underline{k}_m\rangle \langle \underline{n}'| \otimes \sum_{i, \forall s_i=1} \Psi_{m, m', i}^i P_{\underline{n}' + \underline{k}_m, \underline{s} - \underline{s}_i}^{k_p} |\underline{s}\rangle \langle \underline{s}| \right], \quad (\text{A5}) \end{aligned}$$

where $\underline{n} - \underline{k}_m = \underline{n}'$ and the indices in the molecular states have been rearranged.

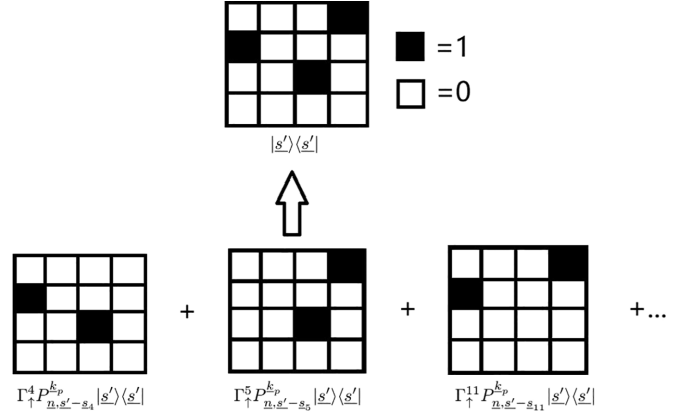


FIG. 5. Visualization of $|\underline{s}'\rangle \langle \underline{s}'|$ as a square, with different contributing terms coming from a set of squares, with one less excitation at position \mathbf{r}_j compared to \underline{s}' . Thus, each term contributes $\Gamma_{\uparrow}^j P_{\underline{n}, \underline{s}' - \underline{s}_j}^{k_p}$.

the same basis $|\underline{n} - \underline{k}_p\rangle \langle \underline{n}| \otimes |\underline{s}\rangle \langle \underline{s}|$, we obtain

$$\dot{P}_{\underline{n}, \underline{s}}^{k_p} \stackrel{L[\sigma_i^+]}{=} \sum_{i, \forall s_i=1} \Gamma_{\uparrow}^i P_{\underline{n}, \underline{s} - \underline{s}_i}^{k_p} - \tilde{\Gamma}_{\uparrow} P_{\underline{n}, \underline{s}}^{k_p}. \quad (\text{A3})$$

The contribution from decay to noncavity modes governed by the Γ_{\downarrow} term can be obtained in a similar manner.

Next, there are the contributions due to the absorption and emission processes, which are given by operators of the $\mathcal{A}_m[\hat{a}_m \hat{\sigma}_i^+ \rho, \hat{a}_m^\dagger \hat{\sigma}_i^-]$ and $\mathcal{E}_{m'}[\hat{a}_{m'}^\dagger \hat{\sigma}_i^- \rho, \hat{a}_{m'} \hat{\sigma}_i^+]$, respectively. For the \mathcal{A}_m term, the relevant relation between the coefficients is

$$\begin{aligned} & \sum_{\underline{n}, \underline{s}} \dot{P}_{\underline{n}, \underline{s}}^{k_p} |\underline{n} - \underline{k}_p\rangle \langle \underline{n}| \otimes |\underline{s}\rangle \langle \underline{s}| \\ & \xrightarrow{\mathcal{A}_m} \frac{1}{2} \sum_{m, m', i} \Psi_{m, m', i}^i \mathcal{A}_{m'} (\hat{a}_m \hat{\sigma}_i^+ \rho \hat{a}_m^\dagger \hat{\sigma}_i^- - \hat{a}_m^\dagger \hat{\sigma}_i^- \hat{a}_m \hat{\sigma}_i^+ \rho). \quad (\text{A4}) \end{aligned}$$

Calculating the first term on the right-hand side gives us the contribution from the term $\hat{a}_m \hat{\sigma}_i^+ \rho \hat{a}_m^\dagger \hat{\sigma}_i^-$:

Similarly, the second term on the right-hand side is the contribution due to $\hat{a}_m^\dagger \hat{\sigma}_i^- \hat{a}_m \hat{\sigma}_i^+ \rho$:

$$\begin{aligned} & \frac{1}{2} \sum_p \Psi_{m,m'}^i \mathcal{A}_{m'} \hat{a}_m^\dagger \hat{\sigma}_i^- \hat{a}_m \hat{\sigma}_i^+ \rho \\ &= \frac{1}{2} \sum_{m,m',\underline{n},\underline{s}} \left[\mathcal{A}_{m'} P_{\underline{n},\underline{s}}^{k_p} \sqrt{(n_m + 1 - \delta_{m,p} - \delta_{m,m'})(n_{m'} - k_{m'})} |\underline{n} - \underline{k}_p - \underline{k}_{m'} + \underline{k}_m\rangle \langle \underline{n} | \otimes \sum_{i,\forall s_i=0} \Psi_{m,m'}^i | \underline{s} \rangle \langle \underline{s} | \right] \end{aligned} \quad (\text{A6})$$

Combining the relations from Eqs. (A5) and (A6), and aligning the corresponding basis, the following expression for the coefficient is obtained:

$$\begin{aligned} \dot{P}_{\underline{n},\underline{s}}^{k_p} \xrightarrow{\mathcal{A}_m} & \frac{1}{2} \sum_{m,m'} \left[\mathcal{A}_{m'} \sqrt{(n_{m'} - \delta_{p,m'} + 1)(n_m + 1)} \left(\sum_{i,\forall s_i=1} \Psi_{m,m'}^i P_{\underline{n}+\underline{k}_m, \underline{s}-\underline{s}_i}^{k_p - k_{m'} + k_m} \right) \right. \\ & \left. - \mathcal{A}_{m'} P_{\underline{n},\underline{s}}^{k_p - k_{m'} + k_m} \sqrt{(n_m + 1 - \delta_{m,p} - \delta_{m,m'})(n_{m'} - k_{m'})} \left(\sum_{i,\forall s_i=0} \Psi_{m,m'}^i \right) \right]. \end{aligned} \quad (\text{A7})$$

The contribution from the Hermitian conjugate and molecular emission, given by the rate $\mathcal{E}_{m'}$ in the master equation, can be calculated along similar lines.

APPENDIX B: DERIVATION OF EQUATION OF MOTION

The detailed derivation of the equation of motion for the photon-photon correlation, using the coefficients arising from the different terms in the master equation, is presented. Again, the terms in the equation arising from \hat{H}_0 and $L[\hat{a}]$ are quite straightforward,

$$\frac{d}{dt} \langle \hat{a}_p^\dagger(t) \hat{a}_q(0) \rangle \xrightarrow{\hat{H}_0} \sum_{\underline{n},\underline{s}} i \delta_p \sqrt{n_p} \dot{P}_{\underline{n},\underline{s}}^{k_p} = i \delta_p \langle \hat{a}_p^\dagger(t) \hat{a}_q(0) \rangle \quad (\text{B1})$$

$$\xrightarrow{L[\hat{a}]} \sum_{\underline{n},\underline{s},m} \kappa \sqrt{n_p} \left[\sqrt{(n_m + 1)(n_m + 1 - \delta_{p,m})} P_{\underline{n}+\underline{k}_m, \underline{s}}^{k_p} - \left(n_m - \frac{1}{2} \delta_{m,p} \right) P_{\underline{n},\underline{s}}^{k_p} \right] \quad (\text{B2})$$

$$= -\frac{1}{2} \sum_{\underline{n},\underline{s}} \kappa \sqrt{n_p} P_{\underline{n},\underline{s}}^{k_p} = -\frac{\kappa}{2} \langle \hat{a}_p^\dagger(t) \hat{a}_q(0) \rangle, \quad (\text{B3})$$

as the $m \neq l$ terms cancel out in the calculation. Next, the contributions from the terms $L[\sigma_i^\pm]$ are considered:

$$\frac{d}{dt} \langle \hat{a}_p^\dagger(t) \hat{a}_q(0) \rangle \xrightarrow{L[\sigma_i^\pm]} \sum_{\underline{n}} \sqrt{n_p} \sum_{\underline{s}} \left\{ \left(\sum_{i,\forall s_i=1} \Gamma_\uparrow^i P_{\underline{n},\underline{s}-\underline{s}_i}^{k_p} \right) - \sum_{i,\forall s_i=0} \Gamma_\uparrow^i P_{\underline{n},\underline{s}}^{k_p} \right\}. \quad (\text{B4})$$

Note in Eq. (B4) that $\sum_{\underline{s}} (\sum_{i,\forall s_i=1} \Gamma_\uparrow^i P_{\underline{n},\underline{s}-\underline{s}_i}^{k_p}) = \sum_{\underline{s}'} c_{\underline{s}'} P_{\underline{n},\underline{s}'}^{k_p}$ is just a linear combination of $P_{\underline{n},\underline{s}'}^{k_p}$. For each \underline{s}' on the right there exists only one term from the left with $\underline{s} = \underline{s}' + \underline{s}_i$ ($\forall s_i = 0$), which then gives $c_{\underline{s}'} = \sum_{i,\forall s_i=0} \Gamma_\uparrow^i$. Including the expression for $c_{\underline{s}'}$ above, the following relation is obtained:

$$\frac{d}{dt} \langle \hat{a}_i^\dagger(t) \hat{a}_j(0) \rangle \xrightarrow{L[\sigma_i^\pm]} 0. \quad (\text{B5})$$

A similar derivation can be done for the contribution from the term $L[\sigma_i^-]$.

The contribution for the absorption and emission, given by the rates \mathcal{A}_m and $\mathcal{E}_{m'}$, respectively, are considered next. First, the term \mathcal{A}_m for the case $m = m'$:

$$\begin{aligned} \frac{d}{dt} \langle \hat{a}_p^\dagger(t) \hat{a}_q(0) \rangle \xrightarrow{\mathcal{A}_m} & \sum_{\underline{n},\underline{s}} \mathcal{A}_p \left[\sqrt{n_p + 1} n_p \left(\sum_{i,\forall s_i=1} |\psi_p^i|^2 P_{\underline{n}+\underline{k}_m, \underline{s}-\underline{s}_i}^{k_p} \right) - \left(n_m - \frac{\delta_{m,p}}{2} \right) P_{\underline{n},\underline{s}}^{k_p} \left(\sum_{i,\forall s_i=0} |\psi_p^i|^2 \right) \right] \\ & + \sum_{\underline{n},\underline{s},m \neq p} \mathcal{A}_m \left[(n_m + 1) \sqrt{n_p} \left(\sum_{i,\forall s_i=1} |\psi_m^i|^2 P_{\underline{n}+\underline{k}_m, \underline{s}-\underline{s}_i}^{k_p} \right) - n_m \sqrt{n_p} P_{\underline{n},\underline{s}}^{k_p} \left(\sum_{i,\forall s_i=0} |\psi_m^i|^2 \right) \right], \end{aligned} \quad (\text{B6})$$

where $|\psi_m^i|^2$ is the squared wave function of cavity mode m . Now, the last two lines in Eq. (B6) are all $m \neq p$ contributions, and by taking $\underline{n}' = \underline{n} + \underline{k}_m$, the last two lines become

$$\sum_{\underline{n}', \underline{s}, m \neq p} \mathcal{A}_m n'_m \sqrt{n_p} \left(\sum_{i, \forall s_i=1} |\psi_m^i|^2 P_{\underline{n}', \underline{s}}^{k_m} \right) - \sum_{\underline{n}, \underline{s}, m \neq p} \mathcal{A}_m n_m \sqrt{n_p} P_{\underline{n}, \underline{s}}^{k_m} \left(\sum_{i, \forall s_i=0} |\psi_m^i|^2 \right). \quad (\text{B7})$$

Similar to the calculations for $L[\sigma_i^\pm]$, the first bracket $\sum_{i, \forall s_i=0} |\psi_m^i|^2$ is transformed to $\sum_{i, \forall s_i=1} |\psi_m^i|^2$, and therefore cancel when $m \neq l$. Therefore, only the $m = p$ terms remain:

$$\frac{d}{dt} \langle \hat{a}_p^\dagger(t) \hat{a}_q(0) \rangle \xrightarrow{\mathcal{A}_m} -\frac{1}{2} \sum_{\underline{n}, \underline{s}} \mathcal{A}_p \sqrt{n_p} P_{\underline{n}, \underline{s}}^{k_p} \times \left(\sum_{i, \forall s_i=0} |\psi_p^i|^2 \right). \quad (\text{B8})$$

For $m \neq m'$:

$$\begin{aligned} \frac{d}{dt} \langle \hat{a}_p^\dagger(t) \hat{a}_q(0) \rangle &\xrightarrow{\mathcal{A}_{m'}} \sum_{\underline{n}, \underline{s}, m \neq m'} \frac{\mathcal{A}_{m'}}{2} \left\{ \sqrt{n_p(n_{m'} - \delta_{p,m'} + 1)(n_m + 1)} \left(\sum_{i, \forall s_i=1} \Psi_{m,m'}^i P_{\underline{n} + \underline{k}_m, \underline{s} - \underline{s}_i}^{k_i - k_{m'} + k_m} \right) \right. \\ &\quad - \sqrt{n_p(n_{m'} - \delta_{p,m'} + 1 - \delta_{m,m'})(n_m - \delta_{m,p})} \left(\sum_{i, \forall s_i=0} \Psi_{m,m'}^i \right) P_{\underline{n}, \underline{s}}^{k_i - k_{m'} + k_m} \\ &\quad \left. + \sqrt{n_p(n_m - \delta_{m,l} + 1)(n_{m'} + 1)} \left(\sum_{i, \forall s_i=1} \Psi_{m,m'}^i P_{\underline{n} + \underline{k}_{m'}, \underline{s} - \underline{s}_i}^{k_i + k_{m'} - k_m} \right) - \sqrt{n_p n_m (n_{m'} + 1 - \delta_{m,m'})} \left(\sum_{i, \forall s_i=0} \Psi_{m,m'}^i \right) P_{\underline{n} + \underline{k}_{m'} - \underline{k}_m, \underline{s}}^{k_i + k_{m'} - k_m} \right\} \\ &\xrightarrow{\mathcal{A}_{m'}} \sum_{\underline{n}, \underline{s}, m \neq m'} \frac{\mathcal{A}_{m'}}{2} \left(\sum_{i, \forall s_i=0} \Psi_{m,m'}^i \right) \left\{ \sqrt{n_p(n_{m'} - \delta_{m',p} + 1)(n_m + 1)} P_{\underline{n} + \underline{k}_m, \underline{s}}^{k_p - k_{m'} + k_m} \right. \\ &\quad - \sqrt{n_p(n_{m'} - \delta_{m',p} + 1 - \delta_{m,m'})} P_{\underline{n}, \underline{s}}^{k_p - k_{m'} + k_m} + \sqrt{n_p(n_m - \delta_{m,i} + 1)(n_{m'} + 1)} P_{\underline{n} + \underline{k}_{m'}, \underline{s}}^{k_p + k_{m'} - k_m} \\ &\quad \left. - \sqrt{n_p n_m (n_{m'} + 1 - \delta_{m,m'})} P_{\underline{n} + \underline{k}_{m'} - \underline{k}_m, \underline{s}}^{k_p + k_{m'} - k_m} \right\}. \quad (\text{B9}) \end{aligned}$$

Rearrangement of some of the indices on the right-hand side of Eq. (B9) gives us

$$\begin{aligned} \frac{d}{dt} \langle \hat{a}_p^\dagger(t) \hat{a}_q(0) \rangle &\xrightarrow{\mathcal{A}_{m'}} \sum_{\underline{n}, \underline{s}, m \neq m'} \frac{\mathcal{A}_{m'}}{2} \left(\sum_{i, \forall s_i=0} \Psi_{m,m'}^i \right) \left\{ \sqrt{(n_p - \delta_{m,p})(n_{m'} - \delta_{p,m'} + 1)n_m} P_{\underline{n}, \underline{s}}^{k_p - k_{m'} + k_m} \right. \\ &\quad - \sqrt{n_p(n_{m'} - \delta_{p,m'} + 1 - \delta_{m,m'})(n_m - \delta_{m,p})} P_{\underline{n}, \underline{s}}^{k_p - k_{m'} + k_m} + \sqrt{(n_p - \delta_{p,m'})(n_m - \delta_{m,p} + 1)n_{m'}} P_{\underline{n}, \underline{s}}^{k_p + k_{m'} - k_m} \\ &\quad \left. - \sqrt{(n_p - \delta_{p,m'} + \delta_{m,p})n_{m'}(n_m + 1 - \delta_{m,m'})} P_{\underline{n}, \underline{s}}^{k_p + k_{m'} - k_m} \right\}. \quad (\text{B10}) \end{aligned}$$

For $m \neq m'$, there can be two cases, either $m = p$ or $m \neq p$, for any m' . For the latter case, $\frac{d}{dt} \langle \hat{a}_p^\dagger(t) \hat{a}_q(0) \rangle = 0$. For $m = p$, the expression is

$$\begin{aligned} \frac{d}{dt} \langle \hat{a}_p^\dagger(t) \hat{a}_q(0) \rangle &\xrightarrow{\mathcal{A}_{m'}} \sum_{\underline{n}, \underline{s}, m=p, m'} \frac{\mathcal{A}_{m'}}{2} \left(\sum_{i, \forall s_i=0} \Psi_{m',p}^i \right) \times \left\{ n_p \sqrt{n_{m'}} P_{\underline{n}, \underline{s}}^{k_{m'}} - (n_p + 1) \sqrt{n_{m'}} P_{\underline{n}, \underline{s}}^{k_{m'}} \right\}, \\ &= \sum_{\underline{n}, \underline{s}, m=p, m'} \frac{-\mathcal{A}_{m'}}{2} \left(\sum_{i, \forall s_i=0} \Psi_{m',p}^i \right) \sqrt{n_{m'}} P_{\underline{n}, \underline{s}}^{k_{m'}}. \quad (\text{B11}) \end{aligned}$$

Again, similar calculations exist for terms arising from emission, \mathcal{E}_m .

APPENDIX C: SEMICLASSICAL APPROXIMATION

The semiclassical approximation used in obtaining the equation of motion in Sec. V is discussed in more detail. The approximation can be written as $P_{\underline{n}, \underline{s}}^{k_m} = P_{\underline{n}}^{k_m} P_{\underline{s}}$, where the probabilities for the photon and molecules are factorized, which implies that the two subsystems are uncorrelated. Moreover, $\sum_{\underline{s}} P_{\underline{s}} = 1$, where $P_{\underline{s}}$ is probability of having excitation profile \underline{s} . Under the

semiclassical approximation we have

$$\langle \hat{a}_p^\dagger(t) \hat{a}_q(0) \rangle = \left(\sum_{\underline{n}} \sqrt{n_p} P_{\underline{n}}^{k_p} \right) \times \left(\sum_{\underline{s}} P_{\underline{s}} \right) = \sum_{\underline{n}} \sqrt{n_p} P_{\underline{n}}^{k_p}. \quad (\text{C1})$$

Applying the approximation in Eq. (C1) to the equation of motion,

$$\begin{aligned} \frac{d}{dt} \langle \hat{a}_p^\dagger(t) \hat{a}_q(0) \rangle &= \left(i\delta_p - \frac{\kappa}{2} \right) \langle \hat{a}_p^\dagger(t) \hat{a}_q(0) \rangle - \sum_m \frac{\mathcal{A}_m}{2} \left(\sum_{\underline{n}} \sqrt{n_m} P_{\underline{n}}^{k_m} \right) \left(\sum_{\underline{s}} \sum_{i, \forall s_i=0} P_{\underline{s}} \Psi_{m,p}^i \right) \\ &+ \sum_m \frac{\mathcal{E}_m}{2} \left(\sum_{\underline{n}} \sqrt{n_m} P_{\underline{n}}^{k_m} \right) \left(\sum_{\underline{s}} \sum_{i, \forall s_i=1} P_{\underline{s}} \Psi_{m,p}^i \right) \\ &= \left(i\delta_p - \frac{\kappa}{2} \right) \langle \hat{a}_p^\dagger(t) \hat{a}_q(0) \rangle - \sum_m \frac{\mathcal{A}_m}{2} \langle \hat{a}_m^\dagger(t) \hat{a}_p(0) \rangle \left[\sum_{\underline{s}} \left(P_{\underline{s}} \sum_{i, \forall s_i=0} \Psi_{m,p}^i \right) \right] \\ &+ \sum_m \frac{\mathcal{E}_m}{2} \langle \hat{a}_m^\dagger(t) \hat{a}_p(0) \rangle \left[\sum_{\underline{s}} \left(P_{\underline{s}} \sum_{i, \forall s_i=1} \Psi_{m,p}^i \right) \right]. \end{aligned} \quad (\text{C2})$$

The term $\sum_{\underline{s}} (P_{\underline{s}} \sum_{i, \forall s_i=1} \Psi_{m,p}^i)$ can be transformed into $\sum_i \Psi_{m,p}^i (\sum_{\underline{s}', \forall s'_i=1} P_{\underline{s}'})$, where the last summation is over all \underline{s}' with unity at position i . The sum $\sum_{\underline{s}'} P_{\underline{s}'}$ is simply the total probability of net excitation of the i th molecule (i.e., the molecules at position \mathbf{r}_i). Using a similar argument, $\sum_{\underline{s}} (P_{\underline{s}} \sum_{i, \forall s_i=0} \Psi_{m,p}^i)$ can be changed to $\sum_i \Psi_{m,p}^i (\sum_{\underline{s}, \forall s_i=0} P_{\underline{s}})$, where $\sum_{\underline{s}} P_{\underline{s}}$ is the net probability of the i th molecule being unexcited. Let f be a vector, where f_i is the excitation fraction at position \mathbf{r}_i , which results in $\sum_i \Psi_{p,m}^i (\sum_{\underline{s}'} P_{\underline{s}'}) = \sum_i f_i \Psi_{p,m}^i$ and $\sum_i \Psi_{p,m}^i (\sum_{\underline{s}} P_{\underline{s}}) = \sum_i (1 - f_i) \Psi_{p,m}^i$.

The equation of motion of the photon-photon correlation under the semiclassical approximation is then given by

$$\frac{d}{dt} \langle \hat{a}_p^\dagger(t) \hat{a}_q(0) \rangle = \left(i\delta_p - \frac{\kappa}{2} \right) \langle \hat{a}_p^\dagger(t) \hat{a}_q(0) \rangle - \frac{1}{2} \sum_{m,i} (\mathcal{A}_m \langle \hat{a}_m^\dagger(t) \hat{a}_p(0) \rangle (1 - f_i) \Psi_{p,m}^i - \mathcal{E}_m \langle \hat{a}_m^\dagger(t) \hat{a}_p(0) \rangle f_i \Psi_{p,m}^i). \quad (\text{C3})$$

-
- [1] W. Ketterle, Nobel lecture: When atoms behave as waves: Bose-Einstein condensation and the atom laser, *Rev. Mod. Phys.* **74**, 1131 (2002).
- [2] L. P. Pitaevskii and S. Stringari, *Bose-Einstein Condensation* (Oxford University, Oxford, 2003).
- [3] J. Kasprzak, M. Richard, S. Kundermann, A. Baas, P. Jembrun, J. M. J. Keeling, F. M. Marchetti, M. H. Szymńska, R. André, J. L. Staehli, V. Savona, P. B. Littlewood, B. Deveaud, and L. S. Dang, Bose-Einstein condensation of exciton polaritons, *Nature (London)* **443**, 409 (2006).
- [4] R. Balili, V. Hartwell, D. Snoke, L. Pfeiffer, and K. West, Bose-Einstein condensation of microcavity polaritons in a trap, *Science* **316**, 1007 (2007).
- [5] J. Klaers, J. Schmitt, F. Vewinger, and M. Weitz, Bose-Einstein condensation of photons in an optical microcavity, *Nature (London)* **468**, 545 (2010).
- [6] J. Marelic and R. A. Nyman, Experimental evidence for inhomogeneous pumping and energy-dependent effects in photon Bose-Einstein condensation, *Phys. Rev. A* **91**, 033813 (2015).
- [7] S. Greveling, K. L. Perrier, and D. van Oosten, Density distribution of a Bose-Einstein condensate of photons in a dye-filled microcavity, *Phys. Rev. A* **98**, 013810 (2018).
- [8] R. C. Schofield, M. Fu, E. Clarke, I. Farrer, A. Trapalis, H. S. Dhar, R. Mukherjee, J. Heffernan, F. Mintert, R. A. Nyman, and R. F. Oulton, Bose-Einstein condensation of light in a semiconductor quantum well microcavity, [arXiv:2306.15314](https://arxiv.org/abs/2306.15314).
- [9] M. R. Andrews, C. G. Townsend, H.-J. Miesner, D. S. Durfee, D. M. Kurn, and W. Ketterle, Observation of interference between two Bose condensates, *Science* **275**, 637 (1997).
- [10] I. Bloch, T. W. Hänsch, and T. Esslinger, Measurement of the spatial coherence of a trapped Bose gas at the phase transition, *Nature (London)* **403**, 166 (2000).
- [11] H. Deng, G. S. Solomon, R. Hey, K. H. Ploog, and Y. Yamamoto, Spatial coherence of a polariton condensate, *Phys. Rev. Lett.* **99**, 126403 (2007).
- [12] J. D. Plumhof, T. Stöferle, L. Mai, U. Scherf, and R. F. Mahrt, Room-temperature Bose-Einstein condensation of cavity exciton-polaritons in a polymer, *Nat. Mater.* **13**, 247 (2014).
- [13] J. Schmitt, T. Damm, D. Dung, C. Wahl, F. Vewinger, J. Klaers, and M. Weitz, Spontaneous symmetry breaking and phase coherence of a photon Bose-Einstein condensate coupled to a reservoir, *Phys. Rev. Lett.* **116**, 033604 (2016).
- [14] J. Marelic, L. F. Zajiczek, H. J. Hesten, K. H. Leung, E. Y. X. Ong, F. Mintert, and R. A. Nyman, Spatiotemporal coherence of non-equilibrium multimode photon condensates, *New J. Phys.* **18**, 103012 (2016).
- [15] T. Damm, D. Dung, F. Vewinger, M. Weitz, and J. Schmitt, First-order spatial coherence measurements in a thermalized two-dimensional photonic quantum gas, *Nat. Commun.* **8**, 158 (2017).
- [16] B. T. Walker, L. C. Flatten, H. J. Hesten, F. Mintert, D. Hunger, A. A. P. Trichet, J. M. Smith, and R. A. Nyman,

- Driven-dissipative non-equilibrium Bose-Einstein condensation of less than ten photons, *Nat. Phys.* **14**, 1173 (2018).
- [17] J. Schmitt, T. Damm, D. Dung, F. Vewinger, J. Klaers, and M. Weitz, Thermalization kinetics of light: From laser dynamics to equilibrium condensation of photons, *Phys. Rev. A* **92**, 011602(R) (2015).
- [18] B. T. Walker, J. D. Rodrigues, H. S. Dhar, R. F. Oulton, F. Mintert, and R. A. Nyman, Non-stationary statistics and formation jitter in transient photon condensation, *Nat Commun.* **11**, 1390 (2020).
- [19] H. S. Dhar, Z. Zuo, J. D. Rodrigues, R. A. Nyman, and F. Mintert, Quest for vortices in photon condensates, *Phys. Rev. A* **104**, L031505 (2021).
- [20] G. Roumpos, M. Lohse, W. H. Nitsche, J. Keeling, M. H. Szymańska, P. B. Littlewood, A. Löffler, S. Höfling, L. Worschech, A. Forchel, and Y. Yamamoto, Power-law decay of the spatial correlation function in exciton-polariton condensates, *Proc. Natl. Acad. Sci. USA* **109**, 6467 (2012).
- [21] I. Carusotto and C. Ciuti, Quantum fluids of light, *Rev. Mod. Phys.* **85**, 299 (2013).
- [22] R. A. Nyman and M. H. Szymańska, Interactions in dye-microcavity photon condensates and the prospects for their observation, *Phys. Rev. A* **89**, 033844 (2014).
- [23] H. Alaeian, M. Schedensack, C. Bartels, D. Peterseim, and M. Weitz, Thermo-optical interactions in a dye-microcavity photon Bose-Einstein condensate, *New J. Phys.* **19**, 115009 (2017).
- [24] D. W. Snoke and S. M. Girvin, Dynamics of phase coherence onset in Bose condensates of photons by incoherent phonon emission, *J. Low Temp. Phys.* **171**, 1 (2013).
- [25] J. Schmitt, T. Damm, D. Dung, F. Vewinger, J. Klaers, and M. Weitz, Observation of grand-canonical number statistics in a photon Bose-Einstein condensate, *Phys. Rev. Lett.* **112**, 030401 (2014).
- [26] P. Kirton and J. Keeling, Nonequilibrium model of photon condensation, *Phys. Rev. Lett.* **111**, 100404 (2013).
- [27] P. Kirton and J. Keeling, Thermalization and breakdown of thermalization in photon condensates, *Phys. Rev. A* **91**, 033826 (2015).
- [28] J. Keeling and P. Kirton, Spatial dynamics, thermalization, and gain clamping in a photon condensate, *Phys. Rev. A* **93**, 013829 (2016).
- [29] H. J. Hesten, R. A. Nyman, and F. Mintert, Decondensation in nonequilibrium photonic condensates: When less is more, *Phys. Rev. Lett.* **120**, 040601 (2018).
- [30] B. T. Walker, H. J. Hesten, H. S. Dhar, R. A. Nyman, and F. Mintert, Noncritical slowing down of photonic condensation, *Phys. Rev. Lett.* **123**, 203602 (2019).
- [31] A. L. Schawlow and C. H. Townes, Infrared and optical masers, *Phys. Rev.* **112**, 1940 (1958).
- [32] R. A. Nyman, Absorption and fluorescence spectra of Rhodamine 6G [Data set], Zenodo (2017), <https://doi.org/10.5281/zenodo.569817>.
- [33] E. H. Kennard, On the thermodynamics of fluorescence, *Phys. Rev.* **11**, 29 (1918).
- [34] E. H. Kennard, On the interaction of radiation with matter and on fluorescent exciting power, *Phys. Rev.* **28**, 672 (1926).
- [35] B. I. Stepanov, Universal relation between the absorption spectra and luminescence spectra of complex molecules, *Dokl. Akad. Nauk SSSR* **112**, 839 (1957) [*Sov. Phys. Dokl.* **2**, 81 (1957)].
- [36] H. J. Carmichael, *An Open System Approach to Quantum Optics*, Lecture Notes in Physics (Springer, New York, 1993).
- [37] C. W. Gardiner and P. Zoller, *Quantum Noise* (Springer, New York, 2000).
- [38] D. F. Walls and G. J. Milburn, *Quantum Optics* (Springer-Verlag, Berlin, 1994).
- [39] Y. Tang, H. S. Dhar, R. F. Oulton, R. A. Nyman, and F. Mintert, companion paper, Breakdown of temporal coherence in photon condensates, *Phys. Rev. Lett.* **132**, 173601 (2024).